S©MR

СИБИРСКИЕ ЭЛЕКТРОННЫЕ
МАТЕМАТИЧЕСКИЕ ИЗВЕСТИЯ
Siberian Electronic Mathematical Reports
http://semr.math.nsc.ru
ISSN 1813-3304

Том 20, № 2, стр. 144–145 (2023) УДК 519.6
https://doi.org/10.33048/semi.2023.20.??? MSC 74S20

MATHEMATICAL MODELING OF CELL PROPAGATION IN THE BODY USING THE REACTION-DIFFUSION EQUATION

K.P. ILINA

Представлено П.П. Петровым

Abstract: The paper presents mathematical modeling of one-dimensional and two-dimensional problems of cell propagation in the body. The finite difference method is applied to solve the Kolmogorov-Petrovskii-Piskunov-Fisher (KPP-F) reaction-diffusion equation. In the one-dimensional case, cell concentration behavior along a finite segment is examined, while the two-dimensional problem enables visualization of the propagation process in a rectangular domain. Numerical implementations of the proposed finite difference schemes reveal the effects of diffusion and reaction coefficients on the speed and shape of the cell propagation front, offering insights into the dynamics of biological processes.

Keywords: reaction-diffusion equation, cell propagation, cell proliferation, implicit finite difference scheme, computational experiment.

1 Introduction

In recent years, mathematical modeling has become an essential tool in biology and medicine, providing insights and descriptions of complex dynamic processes,

Ilina, K.P., Mathematical modeling of cell propagation in the body using the reaction-diffusion equation.

Работа выполнена при финансовой поддержке гранта РНФ No. 23-71-30013(https://rscf.ru/project/23-71-30013/).

Поступила 1 января 2023 г., опубликована 31 декабря 2023 г.

such as wound healing, tumor growth, embryonic development, and cancer cell metastasis. One of the primary methods for modeling these processes is through mathematical models based on reaction-diffusion equations. Of particular significance is the Kolmogorov-Petrovskii-Piskunov-Fisher (KPP-F) equation, which has proven to be a universal tool for analyzing cell migration and proliferation dynamics [1, 2]. This equation has demonstrated remarkable versatility and is widely applied in biology to model cell migration and growth dynamics.

An adult human body consists of approximately thirty trillion cells, each engaged in complex processes of migration, division, and interaction with its surroundings. The KPP-F model effectively describes systems in which cells both migrate through space and proliferate. The diffusion component of the equation captures the tendency of cells to equalize their concentration through random movements, typical of biological systems where cells do not have a defined directional movement but rather disperse across space. The reaction component models population growth, representing biological cell reproduction. However, as in real biological systems, cell population growth is not unlimited. Constraints such as limited nutrients, oxygen, or physical space cause the growth rate to decelerate over time. The nonlinear term in the equation accounts for this saturation effect, modeling how cell mass growth stabilizes as the maximum cell concentration is reached within a bounded area. From the numerical modeling perspective, developing stable difference schemes for solving the KPP-F equation is an important challenge. Some studies propose alternating direction implicit (ADI) schemes, which ensure second-order accuracy in both time and space [24]. Other studies [23] examine globally stable difference schemes that preserve monotonicity and are suitable for a wide range of nonlinear problems.

The class of reaction-diffusion equations under consideration admits traveling wave solutions, which are effectively used to model a variety of invasive phenomena with applications in biology, immunology, ecology, and combustion theory [8], [10]–[18], [25]–[30]. A traveling wavefront forms when there is a balance between diffusion, which acts to spread the substance evenly across space, and the nonlinear reaction, which maintains concentration at a certain level. For example, traveling fronts can be observed in epidemics spreading through populations at a characteristic speed or in combustion, where flames propagate through a combustible substance, preserving a constant wave shape. Biological invasion occurs when populations of reproducing organisms or cells evolve into traveling fronts that invade unoccupied areas. In the context of wound healing, a traveling wave describes how epithelial cells spread from wound edges towards the center, filling the damaged area and regenerating tissue [3, 4]. Another example of biological invasion is tumor invasion, where cancer cells infiltrate tissues or metastasize throughout the body [5, 9, 22]. In embryonic development, cells differentiate and migrate, forming the structures of an organism. Models based on reaction-diffusion equations help us understand how cells interact with their environment and with each other, how they migrate and reproduce, and what factors influence these processes.

In immunology, these models are used to analyze the spread of viruses, immune response, and the dynamics of cellular interactions within tissues. For example, Volpert's work [6], the waves of the immune response to pathogens are studied, which allows for a better understanding of the spatiotemporal dynamics of infection and the immune system's response to external threats. Such models help predict

how the immune system responds to the spread of infectious agents and study the key mechanisms of immune response activation. Another example is the study [7], which simulates the spread of viruses in tissues using diffusion models. This approach allows for the analysis of the dynamics of viral infection and the spread of viral particles in cellular structures, which is important for understanding the mechanisms of infection and the fight against viruses in the body.

This work is dedicated to the numerical study of cell propagation in the body. Numerical modeling of cell propagation dynamics is employed based on the KPP-F reaction-diffusion equation. Particular attention is paid to the study of solutions of the traveling wave type, reflecting dynamic changes in the process of cell propagation. We obtain independent estimates of the parameters D, a, b and the proper wave propagation velocity and confirm that these estimates lead to accurate predictions of modeling the position of the leading edge of the moving front, as well as the dynamics of cell concentration. This work provides a comprehensive understanding in this area and identifies key directions for future research.

The first section presents a literature review on the main approaches to modeling cell propagation. The second section formulates the one-dimensional problem, constructs a finite difference scheme, and presents the results of computational experiments. The third section describes a computational experiment for the two-dimensional problem setup. The fourth section summarizes the findings of the study.

2 One-Dimensional Model

2.1. Problem Statement. We consider an initial-boundary value problem for the Kolmogorov-Petrovskii-Piskunov (Fisher) reaction-diffusion equation describing cell propagation:

$$\frac{\partial u}{\partial t} = D\frac{\partial^2 u}{\partial x^2} + au - bu^2, \quad x \in (-l/2, l/2), \quad t \in (0, T], \tag{1}$$

where t represents time, x denotes spatial coordinates, D is the diffusion coefficient, $a(x,t)$ is the cell growth coefficient, $b(x,t)$ is the saturation coefficient, and $u(x,t)$ is the cell concentration at point x and at time t.

We impose homogeneous Dirichlet boundary conditions:

$$u(-l,t) = u(l,t) = 0, \qquad t \in (0,T], \tag{2}$$

which signify that cell propagation does not reach the boundaries $x = -l/2,\ x = l/2$.

The initial condition is given in the form of a normal distribution:

$$u(x,0) = u_0(x) = \exp(-100x^2), \quad x \in [-l/2, l/2]. \tag{3}$$

2.2. Construction of the Difference Scheme. To numerically solve the formulated reaction-diffusion problem (KPP-F equation) on the rectangular domain $\overline{\Omega}_T$ with boundary and initial conditions, we apply discretization in both time and space.

In the domain $\overline{\Omega}_T$ of the problem (1)–(3), we introduce a rectangular space-time grid with constant steps h and τ:

$$\overline{\omega}_{h\tau} = \overline{\omega}_h \times \overline{\omega}_\tau,$$

$$\overline{\omega}_h = \{x_i = ih - l/2,\ i = 0, 1, \ldots, N;\ h = l/N\},$$

$$\overline{\omega}_\tau = \{t_j = j\tau,\ j = 0, 1, \ldots, M;\ \tau = T/M\}.$$

On the grid $\omega_{h\tau}$, we construct a linear implicit finite difference scheme for the initial-boundary value problem (1)–(3):

$$\begin{cases} \dfrac{u_i^n - u_i^{n-1}}{\tau} = D\dfrac{u_{i-1}^n - 2u_i^n + u_{i+1}^n}{h^2} + au_i^n - bu_i^n u_i^{n-1}, \\ \qquad i = 1, 2, \ldots, N-1, \qquad n = 1, 2, \ldots, M, \\ \qquad u_0^n = u_N^n = 0, \qquad n = 1, 2, \ldots, M, \\ \qquad u_i^0 = u_0(x_i), \qquad i = 0, 1, \ldots, N. \end{cases} \tag{4}$$

2.3. Numerical Results. This section presents the numerical simulation results of cell population propagation within tissue using the KPP-F reaction-diffusion equation. To obtain the numerical solution, we used the finite difference method. The difference scheme (4) was applied to calculate cell concentration values at each time step. Visualization includes graphs demonstrating cell concentration changes at various time points and three-dimensional plots showing the spatio-temporal dynamics of cell propagation.

Numerical calculations were performed with the following parameters: $n = 280$–number of spatial nodes, $m = 180$–number of time steps, $D = 0.001$–diffusion coefficient, $a = 1$–growth coefficient, $b = 1$–saturation coefficient, and $L = 10$–domain length. Figure 1(a) presents graphs of cell concentration $u(x, t)$ as a function of coordinate x for time slices $t_1 = 9.6$, $t_2 = 19.2$, $t_3 = 28.8$, $t_4 = 38.4$, and $t_5 = 48$. The initial state (blue curve) shows a high cell concentration in the center of the domain ($x = 0$). Over time, the diffusion front expands, and cell concentration gradually decreases at the periphery, corresponding to the cell proliferation and propagation process. As time progresses, the wave front becomes wider and less pronounced, characteristic of diffusion processes.

Figure 1(b) shows a three-dimensional visualization of the wavefront dynamics. The initial cell concentration is maximal, and as time progresses, the front propagates at a constant speed, with the overall cell concentration reaching saturation (plateau). This propagation process is typical for reaction-diffusion systems where cell diffusion and growth limitation interact.

These numerical results illustrate how diffusion and reaction interact, creating a wave of cell concentration that expands while the growth stabilizes upon reaching saturation.

2.4. Influence of Growth and Saturation Coefficients. To study the influence of the growth coefficient a and saturation coefficient b, additional numerical experiments were conducted using the same parameters: $n = 280$, $m = 180$, and $L = 10$. Figures 2(a) and 2(b) show the results for $a = 0.5$ and $b = 1$. In this case, saturation significantly affects the cell growth dynamics. Early in the process, cells proliferate actively due to the growth coefficient $a = 0.5$; however, the saturation $b = 1$ quickly slows the growth. The diffusion front continues to expand, but the cell concentration noticeably decreases due to the saturation effect. This reduces the amplitude of the front as the wave advances, which is typical of systems with high saturation: as the maximum cell concentration is reached, growth halts, and the wave front moves at a constant speed.

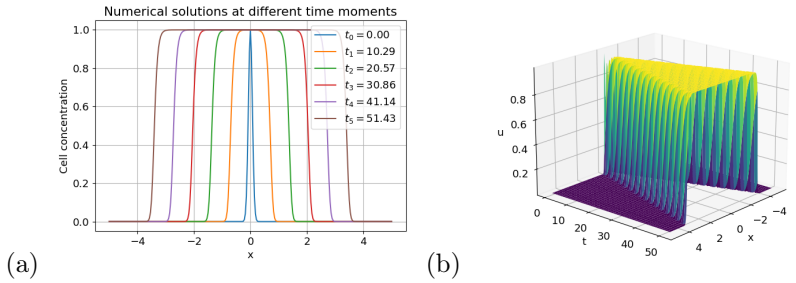

(a) (b)

FIG. 1. Numerical solution with parameters: $D = 0.001, a = 1, b = 1$. (a) Cell concentration $u(x,t)$ variation at different time points. (b) Dynamics of the "traveling wave" in three-dimensional projection.

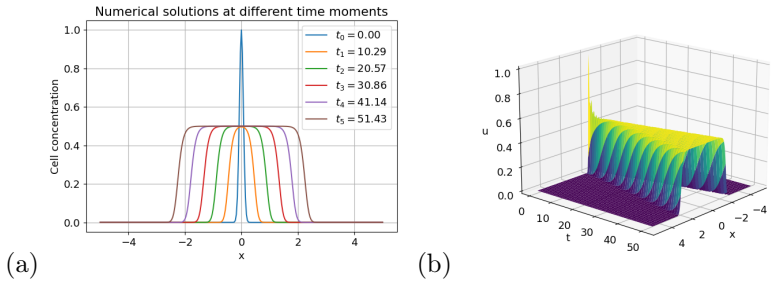

(a) (b)

FIG. 2. Numerical solution with parameters: $D = 0.001, a = 0.5, b = 1$. (a) Cell concentration $u(x,t)$ at different time points. (b) Dynamics of the "traveling wave"in three-dimensional projection.

Figures 3(a) and 3(b) show the results for $a = 0.5$ and $b = 0.1$. With reduced saturation, cells maintain high concentration over a longer period. Although the growth coefficient $a = 0.5$ remains the same, the lower value of b allows the cell population to grow faster and sustain a higher concentration. Numerical results show that the wave front propagates at a higher speed, and the cell concentration remains higher at greater distances from the center. Consequently, the system stabilization process slows, allowing the active front of cell propagation to persist for longer.

Thus, the results show that the saturation coefficient significantly impacts the speed of propagation and the cell concentration front. Low saturation allows cells to maintain higher concentration for longer and accelerates the front's spread, while high saturation limits growth and slows down the propagation process.

2.5. Application to Physical Processes. To model wound healing processes, biologically relevant parameters for cells involved in tissue regeneration (e.g., fibroblasts or epithelial cells) were used. In this task, the growth coefficient a was chosen in the range of 0.1 to 1, reflecting the typical healing process, where cells proliferate to restore damaged tissues. The saturation coefficient b, as in real biological systems,

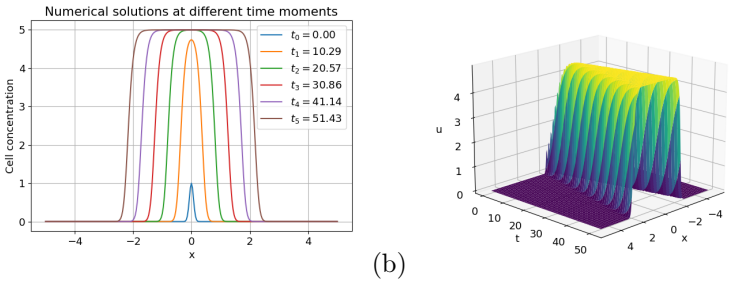

(a) (b)

FIG. 3. Numerical solution with parameters: $D = 0.0001, a = 0.5, b = 0.1$. (a) Cell concentration $u(x,t)$ at different time points. (b) Dynamics of the "traveling wave"in three-dimensional projection.

was selected to be greater than a to model cell growth regulation: as cell density increases, further proliferation is suppressed. Approximate values of b ranged from 0.5 to 2.

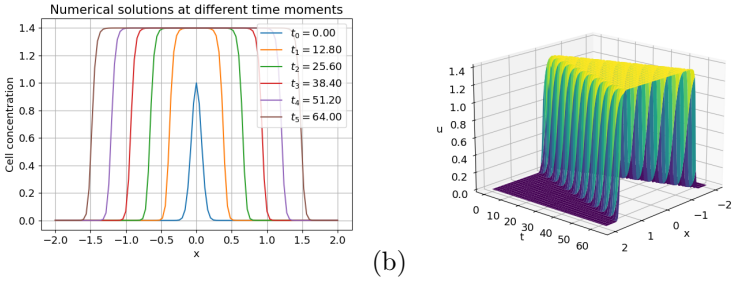

(a) (b)

FIG. 4. Numerical solution with parameters: $D = 0.0001, a = 0.7, b = 0.5$. (a) Cell concentration $u(x,t)$ at different time points. (b) Dynamics of the "traveling wave"in three-dimensional projection.

Figures 4(a) and 4(b) display simulation results for parameters $n = 100$, $m = 200$, $D = 0.0001$, $a = 0.7$, $b = 0.5$, and $L = 4$. The graphs show cell concentration as a function of coordinate x at different time points. Curves of different colors correspond to time slices: $t_1 = 8.53$, $t_2 = 17.07$, $t_3 = 25.6$, $t_4 = 34.13$, and $t_5 = 42.67$. The graphs indicate that cell concentration accumulates in the central region and slowly spreads due to low diffusion. In the early stages of the simulation, cell concentration rises sharply at the center, and then the front gradually moves towards the periphery.

Figure 4(a) illustrates that the cell concentration surface initially increases at the center and then slowly spreads as diffusion takes place, confirming the slow nature of cell mass propagation.

2.6. Analysis of «Traveling Wave» Propagation Speed in the Discrete Problem. Theoretical studies have established that reaction-diffusion systems may exhibit wave solutions with certain speeds under specific conditions. For the

simple or general case of a one-dimensional system, the wave speed v is theoretically defined by the expression $v = 2\sqrt{Da}$, where D is the diffusion coefficient and a is the reaction coefficient [19]–[21].

In this stage, to derive the wave speed formula, we neglect the nonlinear "reaction"term and consider only the diffusion part. It can be noted that the propagation speed of the "traveling wave"depends on diffusion. Numerical modeling discretizes the spatial domain into n grid points with spatial step h and advances in time with a time step τ, determined by the stability condition $\tau = h^2/D$. Thus, the wave propagation speed is calculated as $v = D/h$.

This result shows that the wave front speed increases with the diffusion coefficient, as diffusion accelerates the process of concentration equalization across space. At the same time, finer spatial discretization results in a slower wave front propagation in the numerical model.

3 Two-Dimensional Model

3.1. Problem Statement. Let Ω represent the tissue domain in which we study the cell propagation process. It is assumed that cell propagation in this area occurs under the influence of diffusion and reaction, described by a reaction-diffusion equation of the KPP-Fisher type. In the two-dimensional case, this equation takes the following form:

$$\frac{\partial u}{\partial t} = D\left(\frac{\partial^2 u}{\partial x^2} + \frac{\partial^2 u}{\partial y^2}\right) + au - bu^2, \quad x, y \in \Omega, \quad t \in (0, T], \tag{5}$$

where D is the diffusion coefficient, $a(x, y, t)$ is the cell growth rate, $b(x, y, t)$ is the saturation coefficient, and $u(x, y, t)$ is the cell concentration at point (x, y) at time t.
$\Omega = (0, l_x) \times (0, l_y)$.

We set homogeneous Dirichlet boundary conditions on the boundary of the domain $\partial\Omega$:

$$u(x, y, t) = 0, \quad t \in (0, T]. \tag{6}$$

The studied domain Ω represents a rectangular region that models a section of tissue. Initially, cells are concentrated at the center of this region. The initial condition is set by a normal distribution:

$$u(x, y, 0) = \exp\Big(-100\big((x - 0.5l_x)^2 + (y - 0.5l_y)^2\big)\Big) \quad x, y \in \overline{\Omega}. \tag{7}$$

3.2. Construction of the Finite Difference Scheme. To solve the problem numerically, a rectangular space-time grid is used:

$$\overline{\omega}_{h\tau} = \overline{\omega}_h \times \overline{\omega}_\tau,$$

where

$$\overline{\omega}_h = \{(x_i, y_j) \mid x_i = ih_x,\ y_j = jh_y, \quad i = 0, 1, \ldots, N_x;\ j = 0, 1, \ldots, N_y\},$$

and the spatial steps $h_x = l_x/N_x$ and $h_y = l_y/N_y$ are set by the number of nodes along each axis. The time grid $\overline{\omega}_\tau = \{t_n = n\tau,\ n = 0, 1, \ldots, N_t\}$ is defined with time step $\tau = T/N_t$.

On the grid $\omega_{h\tau}$, we associate the boundary value problem (5) – (7) with the finite difference scheme:

$$\begin{cases} \dfrac{u_{i,j}^n - u_{i,j}^{n-1}}{\tau} = D\left(\dfrac{u_{i-1,j}^n - 2u_{i,j}^n + u_{i+1,j}^n}{{h_x}^2} + \dfrac{u_{i,j-1}^n - 2u_{i,j}^n + u_{i,j+1}^n}{{h_y}^2}\right) + \\ + \quad au_{i,j}^n - bu_{i,j}^n u_{i,j}^{n-1}, \qquad i = 1,2,\ldots,N_x-1, \quad j = 1,2,\ldots,N_y-1, \\ \qquad\qquad n = 1,2,\ldots,N_t, \\ u_{0,j}^n = u_{N_x,j}^n = 0, \quad j = 1,2,\ldots,N_y-1, \quad n = 1,2,\ldots,N_t, \\ u_{i,0}^n = u_{i,N_y}^n = 0, \quad i = 1,2,\ldots,N_x-1, \quad n = 1,2,\ldots,N_t, \\ u_{i,j}^0 = u_0(x_i, y_j), \quad i = 0,1,\ldots,N_x, \quad j = 0,1,\ldots,N_y. \end{cases} \tag{8}$$

3.3. Numerical Results. This section presents the results of numerical modeling of cell propagation in a two-dimensional domain using the discrete scheme (8). The modeling domain is represented by a rectangle $(-l/2; l/2)$ along both axes $(x; y)$. Numerical experiments were performed for two sets of parameters corresponding to different conditions of cell propagation. Visualization of the results is done as contour and 3D plots, allowing observation of the cell propagation dynamics in the studied domain. The contour plots show the two-dimensional distribution of substance at various times, while the 3D plots illustrate the spatial concentration of cells.

The first numerical experiment was performed with parameters $D = 0.001$, $a = 1$, $b = 1$, $l_x = 10$, $l_y = 6$, $N_x = N_y = 280$, $N_t = 180$. These parameters model a system with high diffusion rate and saturation reaction. In Fig. 5 on the left side are contour plots illustrating the spread of cell concentration along the x, y axes at different times: $t = 0$, $T/2$, T. The initial condition sets cell concentration in the center of the domain, and over the modeling process, the cell concentration propagates radially. At time step $t = T/2 = 15.43$, cells actively spread from the center, indicated by increased concentration along the front. At the final time $t = T = 30.86$, the system achieves uniform distribution of cell density across the domain, with cell concentration near zero at the boundaries, consistent with Dirichlet boundary conditions.

On the right side of Fig. 5, 3D plots illustrate cell concentration spread at various times. Initially, the surface shows a distinct peak in the center, indicating high cell concentration. Over time (at intermediate times), this peak spreads and "blurs"due to diffusion and reaction processes. At the final time, the peak nearly disappears, and the surface becomes smoother, indicating an even cell distribution throughout the domain.

The second numerical experiment uses parameters $D = 0.0001$, $a = 0.7$, $b = 0.5$, $l_x = 8$, $l_y = 4$, $N_x = N_y = 100$, $N_t = 200$. Here, conditions approximating biological processes, such as wound healing where cell population saturation occurs more slowly, are modeled. The lower diffusion coefficient and adjusted growth parameters allow cells to maintain high concentration along the wavefront. In Fig. 6, contour plots are shown on the left and 3D plots on the right at different times. At the initial time $t = 0$, cell concentration is concentrated in the center. At the intermediate time step

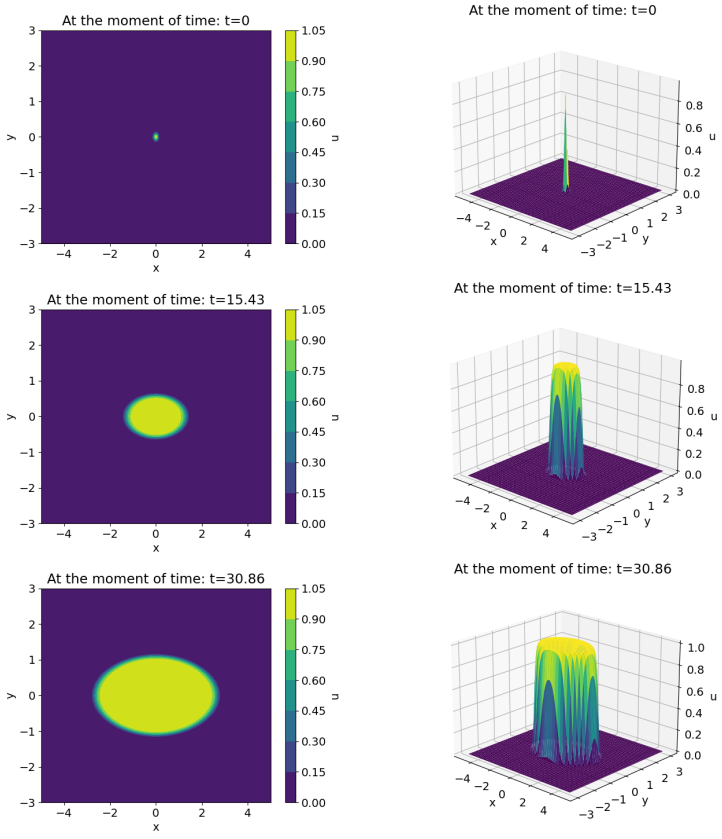

FIG. 5. Dynamics of cell propagation u(x,y,t) at various times in the form of contour and 3D graphs with: $D = 0.001, a = 1, b = 1$

The second numerical experiment uses the parameters $D = 0.0001$, $a = 0.7$, $b = 0.5$, $l_x = 8$, $l_y = 4$, $N_x = N_y = 100$, $N_t = 200$. This simulates conditions similar to biological processes, such as wound healing, where saturation of the cell population occurs more slowly. The lower diffusion coefficient and modified growth parameters allow cells to maintain a high concentration along the wave front. Figure 6 shows contour plots on the left and three-dimensional plots on the right for different moments in time. At the initial moment $t = 0$, the concentration of cells is concentrated at the center. At the intermediate step $t = T/2 = 32$, the cell front spreads across the area, and due to weak saturation, a high concentration of cells is maintained near the front. By the final moment $t = T = 64$, the cells occupy a significant portion of the area, creating a uniform distribution, but the concentration of cells at the boundaries remains low.

The numerical results demonstrate that the concentration of cells concentrated in the center of the area gradually spreads under the influence of diffusion and reaction. At the initial moment, a high concentration of cells is observed in the center, but over time, the wave of cells spreads throughout the area. By the final moment, the concentration at the boundaries approaches zero, which corresponds

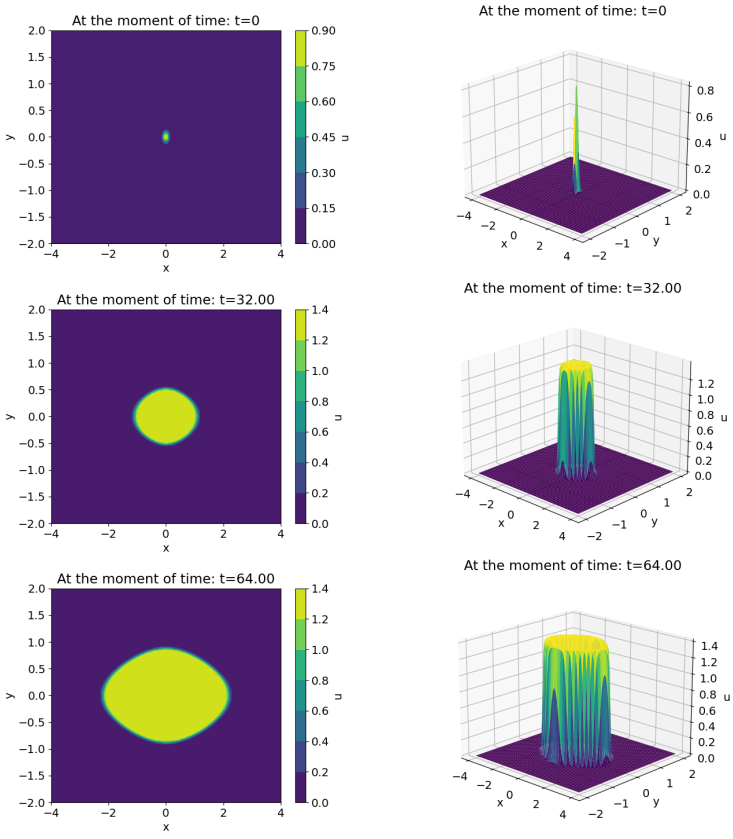

FIG. 6. Dynamics of cell propagation u(x,y,t) at various times in the form of contour and 3D graphs with: $D = 0.0001, a = 0.7, b = 0.5$

to the boundary conditions. Diffusion facilitates the gradual spread of cells, while the reaction ensures population growth followed by saturation.

4 Conclusion

In this work, numerical modeling of cell propagation processes in one-dimensional and two-dimensional settings was conducted using the reaction-diffusion equation of the KPP-F type. The study analyzed the dynamics of cell propagation under the influence of diffusion and reaction, as well as the impact of key model parameters on the speed and characteristics of the cell concentration wave front.

The investigation demonstrated that the one-dimensional model exhibits a strong dependence of the wave front speed of cell concentration on diffusion and growth parameters. At high diffusion coefficients, cells spread more rapidly across the domain, but the wave front becomes less distinct, indicating a redistribution of cell mass and the "blurring"of the propagation boundary. Growth parameters also have a significant effect: in the initial stages, they facilitate the rapid filling of space with

cells; however, the saturation effect gradually slows this process as concentration increases.

The two-dimensional formulation of the problem allowed for a more detailed examination of the spatial behavior of cells. The modeling showed that the initial concentration of cells, concentrated at the center of the domain, spreads symmetrically in all directions, forming a radial wave front that eventually encompasses the entire area. Diffusion plays a key role in the propagation of cells throughout the domain, while growth reactions contribute to a rapid increase in population during the initial time layers. By the end of the simulation, the saturation effect significantly slows down propagation, contributing to the stabilization of cell concentration and the leveling of the distribution.

An important aspect of the approach was also the adaptive management of the time step in the implementation of the numerical method for both one-dimensional and two-dimensional problems. The time step τ was adapted through spatial discretization. The simulation time was not directly specified but calculated as $T = m\tau$, allowing for flexible control of the time interval depending on the grid step. This approach ensured numerical stability and accuracy of the solution when increasing or decreasing the spatial step.

References

[1] A.N. Kolmogorov, I.G. Petrovsky, and N.S. Piskunov, *Investigation of the equation of diffusion combined with increase in the amount of substance and its application to a biological problem*, [in Russian] Mosc. Univ. Math. Bull., **1** (1937), 1–26.

[2] R.A. Fisher, *The wave of advance of advantageous genes*, Annals of eugenics, **7**:4 (1937), 355–369.

[3] A. OHabbal, H. Barelli, G. Malandain, *Assessing the ability of the 2D Fisher–KPP equation to model cell-sheet wound closure*, Mathematical Biosciences, **252** (2014), 45–59.

[4] M.J. Simpson et al., Quantifying the roles of cell motility and cell proliferation in a circular barrier assay, *Journal of the Royal Society Interface*, **10** (2013), 20130007.

[5] J. Perez-Beteta, A. Martinez-Gonzalez, and V.M. Perez-Garcia, A three-dimensional computational analysis of magnetic resonance images characterizes the biological aggressiveness in malignant brain tumours, *Journal of the Royal Society Interface*, **15**:149 (2018), 20180503.

[6] V. Volpert, Existence of Reaction–Diffusion Waves in a Model of Immune Response, *Mediterranean Journal of Mathematics*, **17**:12 (2020), 47.

[7] G. Bocharov et al., Spatiotemporal dynamics of virus infection spreading in tissues, *PLoS One*, **11**:12 (2016), e0168576.

[8] G.A. Bocharov, V.A. Volpert , A.L. Tasevich Reaction-diffusion equations in immunology, *Comput. Math. Math. Phys.*, **58**:12 (2018), 2048–2059.

[9] M.A.J. Chaplain and G. Lolas, Mathematical modelling of cancer invasion of tissue: dynamic heterogeneity, *Amer. Institute Math. Sci.*, **1**:3 (2006), 399–439.

[10] M.V. Shubina, Exact Traveling Wave Solutions of One-Dimensional Models of Cancer Invasion, *J. Appl. Ind. Math.*, **26**:3 (2023), 179–194.

[11] S. Trofimchuk and V. Volpert, Traveling waves in delayed reaction-diffusion equations in biology, *Mathematical Biosciences and Engineering*, **17**:6 (2020), 6487–6514.

[12] YaB. Zeldovich, D.A. Franz-Kamenetsky, Theory of thermal flame propagation, [in Russian] *J. Phys. Chem.*, **19**:9 (1938), 693–697.

[13] Ya.B. Zeldovich, G.I. Barenblatt, V.B. Librovich, G.M. Makhviladze, *Mathematical Theory of Burning and Explosion*, [in Russian] «Nauka» Pub. Mosc., 1980.
[14] J.-G. Caputo and B. Sarels, Reaction-diffusion front crossing a local defect, *Phys. Rev. E*, **84**:4 (2011).
[15] J.D. Murray, *Mathematical biology: I. An introduction*, 2002.
[16] V.V. Gudkov, Traveling Wave Solutions for Two-Component Reaction-Diffusion Systems, [in Russian] *Journal of Computational Mathematics and Mathematical Physics*, **35**:4 (1995), 615–623.
[17] V. Volpert and S. Petrovskii, Reaction–diffusion waves in biology, *Physics of life reviews*, **6**:4 (2009), 267–310.
[18] L.A. Mahiout et al., Infection spreading in cell culture as a reaction-diffusion wave, *ESAIM: Mathematical Modelling and Numerical Analysis*, **56**:3 (2022), 791–814.
[19] N. Bacaër, *A short history of mathematical population dynamics*, Springer-Verlag London Limited, 2011.
[20] M. El-Hachem et al., Revisiting the Fisher–Kolmogorov–Petrovsky–Piskunov equation to interpret the spreading–extinction dichotomy, *Proceedings of the Royal Society A*, **475**:2229 (2019), 20190378.
[21] G.C. Paul et al., Revisiting Fisher-KPP model to interpret the spatial spreading of invasive cell population in biology, *Heliyon*, **8**:10 (2022), 10.
[22] A.V. Kolobov, V.V. Gubernov, A.A. Polezhaev, Fisher type waves in a model of invasive tumor growth, *Matem. Mod.*, **19**:6 (2007), 31–42.
[23] P.P. Matus, D. Pylak, ЬUnconditionally monotone and globally stable difference schemes for the Fisher equation, [in Russian] *Reports of the National Academy of Sciences of Belarus*, **67**:6 (2024), 454–459.
[24] S. Kwak et al., An unconditionally stable difference scheme for the two?dimensional modified Fisher–Kolmogorov–Petrovsky–Piscounov equation, *Journal of Mathematics*, **2023**:1 (2023), 5527728.
[25] V.I. Bykov, On the design of computational experiment in combustion theory, *Russian Journal of Physical Chemistry B*, **6** (2012), 289–292.
[26] T.A. Zvonareva, S.I. Kabanikhin, and O.I. Krivorotko, Numerical algorithm for source determination in a diffusion–logistic model from integral data based on tensor optimization, *Computational Mathematics and Mathematical Physics*, **63**:9 (2023), 1654–1663.
[27] T.A. Kandryukova, Y.M. Laevskii, Simulating the filtration combustion of gases on multi-core computers, *Journal of Applied and Industrial Mathematics*, **8** (2014), 218–226.
[28] Y.M. Laevsky, V.S. Babkin, On the theory of a travelling hybrid wave, *Combustion Science and Technology*, **164**:1 (2001), 124–144.
[29] S.V. Aleshin, S.D. Glyzin, S.A. Kaschenko, Fisher–Kolmogorov–Petrovskii–Piscounov Equation with Delay, [in Russian] *Modeling and Analysis of Information Systems*, **22**:2 (2015), 304–321.
[30] A.V. Borisov et al., Numerical simulation of the one-dimensional population dynamics with nonlocal interaction,[in Russian] *Bulletin of the Tomsk Polytechnic University, Geo Assets Engineering*, **315**:2 (2009).

Kiunnei Pavlovna Ilina
North-Eastern Federal University,
Kulakovsky str., 42,
677000, Yakutsk, Russia
Email address: ilina_kunnei@mail.ru